The reversal of the multi-decadal trends of the equatorial Pacific easterly winds, and the Indonesian Throughflow and Leeuwin Current transports

Ming Feng[1], Claus Böning[2], Arne Biastoch[2], Erik Behrens[2], Evan Weller[1], Yukio Masumoto[3,4]

[1]CSIRO Marine and Atmospheric Research, Floreat, Western Australia, Australia

[2]Leibniz-Institut für Meereswissenschaften, Kiel, Germany

[3]Frontier Research Center for Global Change, JAMSTEC, Yokohama, Japan

[4]Department of Earth and Planetary Science, University of Tokyo, Tokyo, Japan

Abstract

Multi-decadal weakening trend of the equatorial Pacific easterly winds since 1960 has reversed after 1993. The trend reversal has induced cooling (shallow thermocline) trend in the equatorial western Pacific before 1993, followed by a warming (deep thermocline) trend from 1993 to the present. All available atmospheric reanalysis products corroborate the trend reversal during the two multi-decadal periods. The magnitudes of the multi-decadal trends of the easterly winds, however, differ among the reanalysis products. The trend reversals of regional ocean circulations are assessed using linear regressions between wind and transport anomalies in an eddy-permitting numerical model, suggesting that since 1993 the Indonesian Throughflow and the Leeuwin Current transports have also reversed their multi-decadal weakening trends.

1. Introduction

Tropical Pacific experienced a sharp climatic regime shift in mid-1970's [Trenberth, 1990; Graham, 1995], followed by more frequent El Niño conditions (negative Southern Oscillation Index, SOI) and positive phase of the Pacific Decadal Oscillation (PDO) (Figure 1a). Associated with the climate regime shift was a multi-decadal weakening trend of easterly winds over the equatorial Pacific from 1960's to early-1990's (Figure 1b), which was coupled with shallow thermocline anomalies in the equatorial western Pacific Ocean and the slowdown of the Pacific subtropical cells [McPhaden and Zhang, 2002; Vecchi et al. 2006]. The shallow thermocline anomalies in the western Pacific Ocean transmitted into the southeastern Indian Ocean and caused subsurface cooling off the northwest coast of Australia and a slowdown of the Indonesian Throughflow (ITF) [Wainwright et al., 2008] and the Leeuwin Current (LC) [Feng et al., 2004].

The tropical Pacific appears to be experiencing another climate regime shift since early-1990's, or a recovery from the earlier shift, with near-neutral SOI and PDO indices (Figure 1a). The equatorial Pacific easterly winds have rejuvenated and experienced a multi-decadal strengthening trend since early-1990's (Figure 1b) [Feng et al., 2010]. There have been reports on the recovery of the strength of the Pacific subtropical cells during the period of early-1990's to early-2000's [McPhaden and Zhang, 2004]. Recent observations of altimeter and coastal sea levels indicate that the reversal of the multi-decadal trends in the tropical Pacific Ocean has sustained over the past decade [Feng et al., 2010; Figure 1c]. It is crucial to quantify the magnitude of these multi-decadal trends and their influences on regional ocean circulations, in order to better assess regional impacts of human-induced climate change.

In this study, multi-decadal trends of the equatorial Pacific winds and their influences on the ITF and the LC are investigated using available atmospheric reanalysis products and an eddy-permitting numerical model, ORCA025 [Biastoch et al. 2008].

2. Data and method

Equatorial Pacific wind stresses are derived from National Center for Environment Prediction (NCEP) and European Center for Medium range Weather Forecast (ECMWF) reanalysis products. The NCEP National Center for Atmospheric Research (NCAR) reanalysis, or NCEP-1, spans 1948 to present [Kalnay *et al*. 1996]. The NCEP Department of Energy reanalysis, or NCEP-2, fixes errors in the NCEP-1 observational database along with other model improvement and provides reanalysis fields from 1979 to present [Kanamitsu *et al*., 2002]. They employ fixed error 3-dimensional variational assimilation techniques, assimilate all independent observations and use ERSST [Smith and Reynolds, 2004] as boundary conditions. The NCEP 20th Century reanalysis (NCEP-20C) utilizes an Ensemble Filter data assimilation system, a new version of the NCEP atmosphere-land model to generate first guess fields with interpolated monthly HadISST sea surface temperature and sea ice concentration fields [Rayner et al., 2003] as prescribed boundary conditions, to produce a reanalysis dataset spanning 1871 to the present [Compo et al., 2011]. ERA-40 is an ECMWF re-analysis of the global atmosphere and surface conditions over the period from 1957 through 2002. Many sources of the meteorological observations were used, and the ERSST is used as the boundary condition. The ECMWF interim reanalysis product is a near realtime extension of ERA-40 from 1989 to present.

Monthly values from an ORCA025, a global implementation of the OPA ocean models [Madec, 2007], version of the NEMO model with a horizontal resolution of 0.25° in the longitudinal direction at the equator [Biastoch *et al*., 2008], are used in this study. The ORCA025 forcing fields are “merged products” of the NCEP-1 reanalysis and various observational (e.g., satellite) products, which are adjusted so as to provide a globally balanced forcing ensemble, the so-called “CORE” forcing [Large, 2007]. In particular, the CORE forcing has corrected the known low bias in the NCEP-1 wind speed [Smith *et al*., 2001] by applying a spatially-dependent factor derived from comparisons with Quick Scatterometer (QuikSCAT) wind, resulting in an increase of ~30% for the wind stress over the equatorial Pacific [Large, 2007; e.g. Figure 3a]. In ORCA025 model output, the ITF transport is defined as the net southward transport through the Indonesian Archipelago in the upper 500 m and monthly-mean LC transport is defined as the net southward transport between 110°E and the west coast of Australia in the top 250 m at 32°S.

Gridded temperature anomaly fields, after correcting for instrumental biases of bathythermograph data and correcting or excluding some Argo float data [Levitus *et al*., 2009], are obtained from National Oceanographic Data Center (NODC). Fremantle sea level is supplied by Australia National Tidal Facility. SOI and PDO indices are obtained from KNMI Climate Explorer.

3. Multi-decadal trends of equatorial Pacific wind stresses

Equatorial zonal wind is closely coupled with zonal sea surface temperature gradient along the equatorial Pacific due to the Bjerknes feedback. It is also closely coupled with the zonal sea level (thermocline depth) gradient based on the Sverdrup balance. Equatorial wind anomalies are often associated with anomalies in off-equatorial wind stress curls, which in turn drive off-equatorial Rossby waves and affect the shallow meridional overturning cells in the Pacific, the subtropical cells. To quantify the magnitude of multi-decadal trends reversal of easterly winds in the equatorial Pacific, two multi-decadal periods: 1960-1993 and 1993-present are determined from the low-pass filtered Fremantle sea level, which is highly correlated with decadal climate variability in the equatorial Pacific [Feng et al., 2010].

All available atmospheric reanalysis products corroborate the trend reversal in the equatorial Pacific prior and after 1993; however, the reanalysis products differ on the magnitude of the trends of the easterly winds during the two multi-decadal periods (Figure 1b; Table 1). NCEP-1 has the strongest weakening trend of during 1960–1993 and has the weakest strengthening trend during 1993–-2008. NCEP-20C and ERA-40 have comparable weakening trend of equatorial winds during 1960–-1993, both have weakened by about 8 × 10^{-3} Nm^{-2} as derived from linear regression with time. While the easterly winds in both NCEP-2 and ECMWF-interim have strengthened by about -8 × 10^{-3} Nm^{-2} during 1993–2008, NCEP-20C has the highest strengthening trend (Table 1). Compared with NCEP-1, CORE forcing has a ~30% stronger weakening trend during 1960-1993, but has a slightly weaker strengthening trend during 1993-2008 (Table 1).

After removing a linear trend of global sea level rise of 1.5 mm $year^{-1}$ [e.g. Church et al., 2004] the low-pass-filtered Fremantle sea level has a steady declining trend from 1960's to early 1990's, followed by a full rebound after early 1990's (Fig. 1c). As the decadal variability of the Fremantle sea level off the west coast of Australia to a large extent reflects the zonal wind variability along the equatorial Pacific [Feng et al. 2004; 2010], the multi-decadal variations of the Fremantle sea level corroborate that there has been a full reversal (recovery) of the easterlies along the equatorial Pacific.

4. Multi-decadal temperature trends in observations

In response to the weakening trend of trade winds, upper ocean (0-300 m) temperature in the equatorial western Pacific cooled by more than 1°C during 1960-1993 (Figures 2a), due to shoaling of the thermocline depth by 10-20 m (not shown), consistent with the slowdown of the Pacific subtropical cells.

Between 1993 and 2008, the Ekman pumping associated with the strengthening of the Pacific easterly winds has generated off-equatorial downwelling Rossby wave-like responses in the western-central Pacific, causing >1°C warming tendency in the upper ocean (Figure 2b). This has largely reversed the cooling trend during the previous decades, and consistent with the faster sea-level rise trend in the western Pacific during the same period [Merrifield et al., 2009; Feng *et al*., 2010] and a rebound of the strength of the Pacific subtropical cells.

The transmission of thermocline anomalies into the southeast Indian Ocean has been captured in the Fremantle sea level data [Feng *et al*., 2010], although they are not well depicted in Figure 2, either due to the smoothing of the gridded dataset or vertical propagation of the temperature signals along the coastal waveguide.

5. Multi-decadal trends in ORCA025

As in linear wave dynamics, there is a good correlation between the annual mean easterly wind stress anomalies and the zonal steric height differences between western and eastern equatorial Pacific, 0.93, in ORCA025 model simulation. Essentially, the annual mean zonal steric height differences in ORCA025 match up rather well with those derived from NODC observations, with a linear correlation of 0.95 (Figure 3b). There are also high correlations between the equatorial Pacific easterly wind anomalies and the ITF and LC transports (Table 2), suggesting that the interannual variability of the ITF and the LC are also to a large extent determined by linear wave dynamics.

On multi-decadal time scale, ORCA025 has higher reduction of the zonal steric height gradient during 1960-1993, while has lower recovery trend during 1993-2008, compared to NODC data (Table 3), consistent with the multi-decadal trends of the NCEP-1/CORE wind forcing.

Multi-decadal trends are evident in the low-pass-filtered time series of the ITF and LC transports from ORCA025 (Figure 3c). The reductions in the ITF and LC transports are 4.7 and 1.9 Sv respectively during 1960-1993, however, there are no significant recovery trends in both the ITF and LC transports after 1993 (Table 4). In a half-degree-resolution ORCA simulation forced by repeated climatology forcing, which is used as a control run of ORCA025, the ITF transport (0-500m) has a weakening drift of 1.5 Sv in 60 years (not shown). The discrepancy between the model simulated trends and those derived from linear regression with winds suggest that ORCA025 may have a higher drift rate compared to the lower resolution control simulation. Despite the model drift, the more significant response of the ITF and LC transports, compared with the steric height along the equator, has raised the possibility that the ITF and LC transports are also sensitive to the off-equatorial sea level anomalies on decadal time scale, driven by anomalous wind stress curls.

For ocean circulation systems that are influenced by linear equatorial waves, such as the ITF and LC, multi-decadal trends can be derived from linear regressions between the transport anomalies and the average zonal wind stresses along the equatorial Pacific, in order to overcome the model drift. Note there are only minor differences in the linear regression coefficients for different multi-decadal periods (Table 2). Using linear regression coefficients derived from ORCA025 for the whole period (Table 2) and linear trends of easterly winds (Table 1), most of the available reanalysis products tend to suggest that linear reductions of the ITF and the LC are 1.5 and 0.7 Sv respectively during 1960-1993 and their strengths have fully recovered during 1993-2008 (Table 4). Note that the total transport of the ITF appears to have strengthened from about 12 Sv as derived from historical measurements spanning 1984-1996 to about 15 Sv during 2004-2006 [Figure 3c; Sprintall et al., 2009].

6. Discussion

Available Intergovernmental Panel of Climate Change Forth Assessment climate models depict a good linear relationship between the strength of the equatorial Pacific easterly winds and the ITF transport (Figure S1; Table S1). All the models, with and without all greenhouse gases (e.g. CO2, CH4, N20, halo carbons), ozone and sulphate aerosols forcing, do not produce multi-decadal variations of the Pacific trade winds that can mimic the multi-decadal trends of the Pacific trade winds before and after the early 1990’s (Figure S2). Although the aerosols forcing is a key driver of decadal variations of heat content anomalies at global scale (e.g. Domingues et al. 2008), it is unlikely responsible for the multi-decadal trend reversal of heat content anomalies in the tropical Pacific. It is most likely that the multi-decadal trends in observations are due to internal variability of the coupled atmosphere-ocean system. Thus, natural climate variability in the tropical Pacific may either exacerbate or lessen the impacts of human-induced climate change on ocean circulations during different decades.

While for circulation systems that are influenced by the linear wave dynamics, their multi-decadal trends can be assessed using linear regression; for processes that involve non-linear ocean dynamics, such as the subtropical cells, however, it is important to have the correct wind forcing in order to hindcast their multi-decadal trends. On the one hand, off-equatorial Rossby waves take longer time to adjust to equilibrium, and on the other hand processes involving subduction and upwelling of water masses may not be cancelled out even when the wind forcing is reversed. Given the discrepancy among different atmospheric reanalysis products, consensus of the forcing fields is necessary in order to evaluate multi-decadal trends of ocean currents and their feedbacks to the atmosphere.

Acknowledgements

This research is partly supported by the Western Australia Marine Science Institution and the Commonwealth Scientific and Industrial Research Organisation (CSIRO) Wealth from Oceans National Research Flagship. We would like to thank Gary Meyers, Jérôme Vialard, Catia Domingues, and two anonymous reviewers for constructive comments.

References:

Biastoch, A., C. W. Böning, J. Getzlaff, J.-M. Molines, and G. Madec (2008), Mechanisms of interannual-decadal variability in the meridional overturning circulation of the mid-latitude North Atlantic Ocean, *J. Climate*, *21*, doi: 10.1175/2008JCLI2404.1, 6599–6615.

Compo, G.P., et al. 2011: The Twentieth Century Reanalysis Project. Quart. J. Roy. Meteor. Soc., 137, 1-28.

Church, J. A., N. J. White, R. Coleman, K. Lambeck, and J. X. Mitrovica (2004), Estimates of the regional distribution of sea level rise over the 1950-2000 period, *J. Climate*, *17*, 2609-2625.

Domingues, C.M. , J.A. Church, N.J. White, P.J. Gleckler, S.E. Wijffels, P.M. Barker and J.R. Dunn (2008), Improved estimates of upper-ocean warming and multi-decadal sea-level rise. *Nature*, **453**, 1090-1094, doi:10.1038/nature07080.

Feng, M., Y. Li, and G. Meyers (2004), Multidecadal variations of Fremantle sea level: footprint of climate variability in the tropical Pacific. *Geophys. Res. Lett.*, *31*: L16302, doi: 10.1029/2004GL019947.

Feng, M., A. Biastoch, C. Boning, N. Caputi, G. Meyers (2008), Seasonal and interannual variations of upper ocean heat balance off the west coast of Australia, *Journal of Geophysical Research*, 113, C12025, doi:10.1029/2008JC004908.

Feng, M., M. J. McPhaden, and T. Lee (2010), Decadal variability of the Pacific subtropical cells and their influence on the southeast Indian Ocean, *Geophys. Res. Lett.*, *37*, L09606, doi:10.1029/2010GL042796.

Graham, N. E. (1995), Simulation of recent global temperature trends, *Science*, 267, 666-671.

Kalnay, E. *et al*. (1996), The NCEP/NCAR 40-year reanalysis project, *Bull. Am. Meteorol. Soc.*, *77*, 437-471.

Kanamitsu, M., et al. (2002), NCEP–DOE AMIP-II Reanalysis (R-2), *Bull. Amer. Meteor. Soc*., 83, 1631–1643.

Large, W. G. (2007), Core Forcing for Coupled Ocean and Sea - Ice Models, *WGSF/WCRP Flux News*, *3*, 2–3.

Levitus, S. et al. (2009), Global ocean heat content 1955–2008 in light of recently revealed instrumentation problems, *Geophys. Res. Lett.*, 36, L07608, doi:10.1029/2008GL037155.

Madec, G. (2007), NEMO: the OPA ocean engine, Note du Pole de Mod’elisation, Institut Pierre-simon Laplace (IPSL), France.

McPhaden, M. J., and D. Zhang (2002), Slowdown of the meridional overturning circulation in the upper Pacific Ocean, *Nature*, *415*, 603-608.

McPhaden, M. J., and D. Zhang (2004), Pacific Ocean circulation rebounds, *Geophys. Res. Lett.*, *31*, L18301, doi:10.1029/2004GL020727.

Merrifield, M. A., S. T. Merrifield, G. T. Mitchum (2009), An Anomalous Recent Acceleration of Global Sea Level Rise, *J. Climate*, **22**, 5772–5781.

Meyers, G. (1996), Variation of Indonesian Throughflow and the El Niño – Southern Oscillation, *J. Geophys. Res.*, *101(C5)*, 12255-12263.

Rayner, N.A., et al. (2003), Globally complete analyses of sea surface temperature, sea ice and night marine air temperature, 1871-2000, *J. Geophys. Res.* 108, 4407, doi 10.1029/2002JD002670.

Smith, S. R., D. M. Legler, and K. V. Verzone (2001), Quantifying Uncertainties in NCEP Reanalyses Using High-Quality Research Vessel Observations, *Journal of Climate*, *14*, 4062–4072.

Smith, T. M., and R. W. Reynolds (2004), Improved extended reconstruction of SST (1854–1997), J. Clim., 17, 2466–2477, doi:10.1175/1520-0442(2004)017<2466:IEROS>2.0.CO;2.

Sprintall, J., S. E. Wijffels, R. Molcard, and I. Jaya (2009), Direct estimates of the Indonesian Throughflow entering the Indian Ocean: 2004–2006, *J. Geophys. Res.*, *114*, C07001, doi:10.1029/2008JC005257.

Trenberth, K. E. (1990), Recent observed decadal climate changes in the Northern Hemisphere, *Bull. Am. Meterological. Soc.*, *71*, 988-993.

Vecchi, G. A., et al. (2006), Weakening of tropical Pacific atmospheric circulation due to anthropogenic forcing, *Nature*, *441*, 73-76, doi:10.1038/nature04744.

Wainwright, L., G. Meyers, S. Wijffels, and L. Pigot (2008), Change in the Indonesian Throughflow with the climatic shift of 1976/77, *Geophysical Research Letters*, *35*, L03604, doi: 10.1029/2007GL031911.

Table 1: Linear changes of easterly wind stress along the equatorial Pacific (averaged over 5°S – 5°N, 120°E – 100°W) in different atmospheric reanalysis products (unit: 10^{-3} Nm^{-2}). The numbers in the parentheses are standard errors of the linear changes determined from a bootstrap method.

	1960-1993	1993-2008
CORE	16.5 (2.6)	-5.6 (4.0)
NCEP-1	12.9 (1.7)	-6.4 (2.8)
NCEP-2	--	-8.1 (2.8)
NCEP-20C	8.4 (2.1)	-11.5 (3.3)
ERA40	7.6 (2.6)	--
ECMWF interim	--	-7.8 (3.4)

Table 2: Linear correlations and regressions with easterly wind stress anomalies along the equatorial Pacific in ORCA025. The regression coefficients are also calculated for the two multi-decadal periods. The model drift is not removed when calculating the regression coefficients.

	Zonal steric height difference	ITF transport	LC transport
Correlation	0.93	0.80	0.79
Regression	1.12 m^2s^{-2} / Nm^{-2}	1.96 Sv / 0.01 Nm^{-2}	0.90 Sv / 0.01 Nm^{-2}
Regression (1960-1993)	1.14 m^2s^{-2} / Nm^{-2}	2.14 Sv / 0.01 Nm^{-2}	0.93 Sv / 0.01 Nm^{-2}
Regression (1993-2008)	1.45 m^2s^{-2} / Nm^{-2}	1.97 Sv / 0.01 Nm^{-2}	0.94 Sv / 0.01 Nm^{-2}

Table 3: Linear changes in zonal steric height differences between the equatorial western and eastern Pacific

	1960-1993	1993-2007
ORCA025	-1.5 (0.4)	0.8 (0.6)
WOD	-1.3 (0.7)	1.1 (0.6)*

*1993-2008

Table 4: Multi-decadal trends of the volume transport of the ITF and LC in ORCA025 model simulation and those estimated from linear trends of the equatorial Pacific easterly winds in available reanalysis products and linear regressions between ORCA025 transports and easterly wind anomalies. The numbers in the parentheses are standard errors.

	Indonesian Throughflow (Sv)		Leeuwin Current (Sv)	
	1960-1993	1993-2008	1960-1993	1993-2008
ORCA025	4.7 (0.7)	-0.6 (1.3)	1.9 (0.4)	0.4 (0.6)
CORE	3.2 (0.5)	-1.1 (0.8)	1.5 (0.2)	-0.5 (0.4)
NCEP-1	2.5 (0.3)	-1.3 (0.5)	1.2 (0.2)	-0.6 (0.3)
NCEP-2	--	-1.6 (0.3)	--	-0.7 (0.3)
NCEP-20C	1.6 (0.4)	-2.3 (0.6)	0.8 (0.2)	-1.0 (0.3)
ERA40	1.5 (0.5)	--	0.7 (0.2)	--
ECMWF interim	--	-1.5 (0.7)	--	-0.7 (0.3)

Figure 1: (a) Annual mean PDO and SOI indices; (b) annual mean zonal wind stress along equatorial Pacific (averaged over 5°S-5°N, 130°E-100°W) derived from different atmospheric reanalysis products, and (c) annual mean detrended Fremantle sea level anomalies. The heavy lines in three panels are smoothed with a 9-year Hanning filter.

Figure 2: Liner trends of 0-300 m vertically averaged NODC temperature anomalies in the tropical Pacific and Indian oceans: (a) during 1960-1993; and (b) during 1993-2009. The units are temperature changes derived from linear trends over the designated periods, *e.g.*, linear trends multiplying the time intervals.

Figure 3: (a) Annual mean zonal wind stress of ORCA025 (CORE forcing) averaged over 5°S-5°N, 130°E-100°W, (b) annual mean zonal surface steric height difference between west Pacific and east Pacific) reference to 500 m in ORCA025, and that derived from NODC temperature fields, and (c) annual mean transports of the ITF and (d) the LC from ORCA025 model simulation. The heavy curves are smoothed using a 9-year Hanning filter. The star and pentagon in (c) denote the ITF transports estimated from historical measurements and from a 2004-2006 monitoring project [derived from Table 1 in Sprintall et al., 2009].

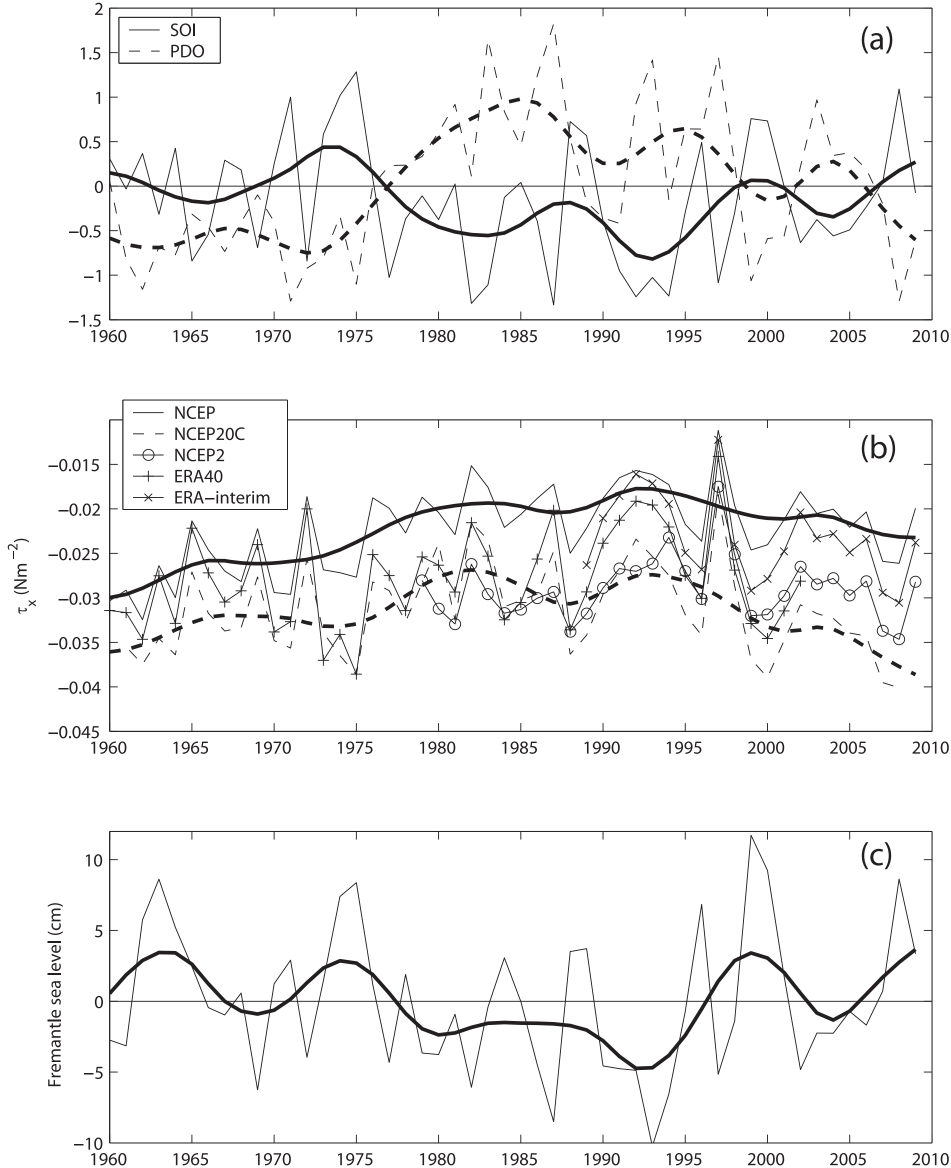

SOI
PDO
(a)
NCEP
NCEP20C
NCEP2
ERA40
ERA−interim
(b)
τ_x (Nm^{-2})
(c)
Fremantle sea level (cm)

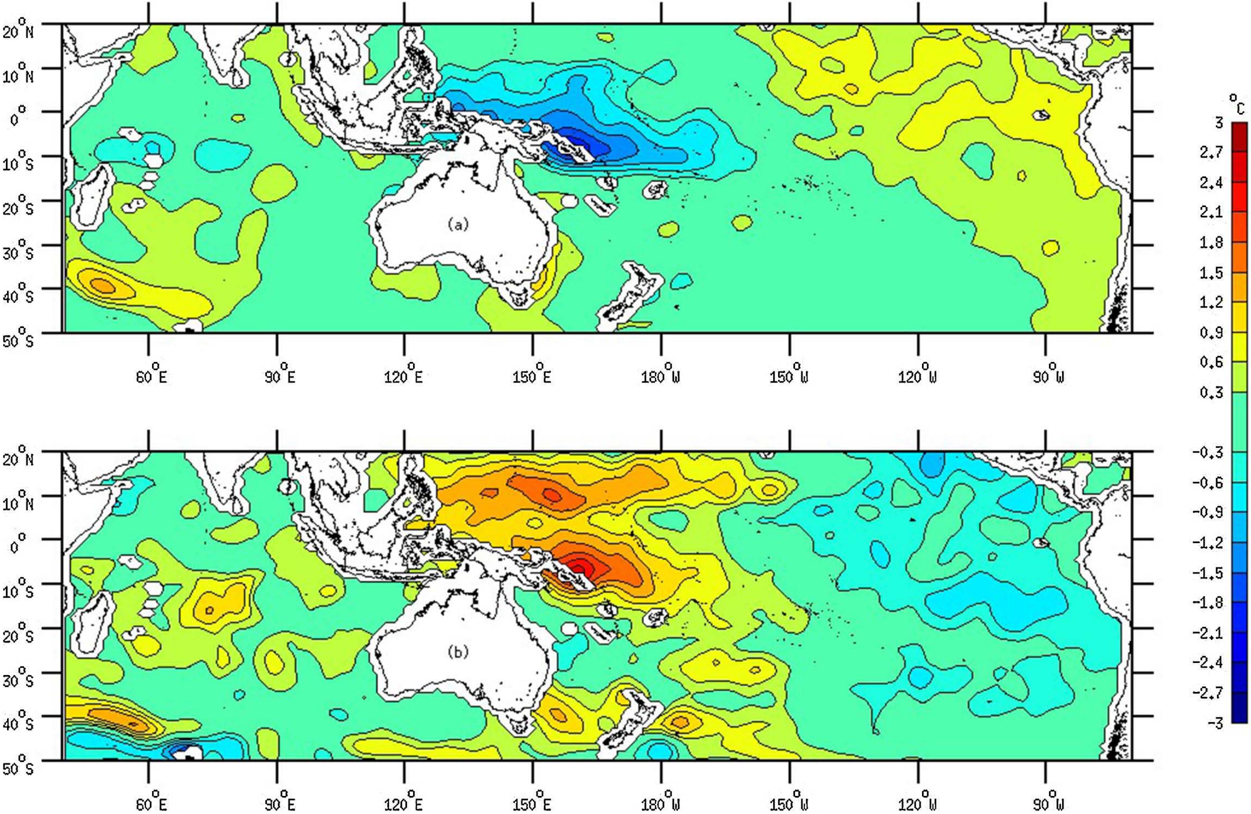
20°N
10°N
0°
10°S
20°S
30°S
40°S
50°S
60°E
90°E
120°E
150°E
180°W
150°W
120°W
90°W
(a)
(b)
°C
3
2.7
2.4
2.1
1.8
1.5
1.2
0.9
0.6
0.3
-0.3
-0.6
-0.9
-1.2
-1.5
-1.8
-2.1
-2.4
-2.7
-3

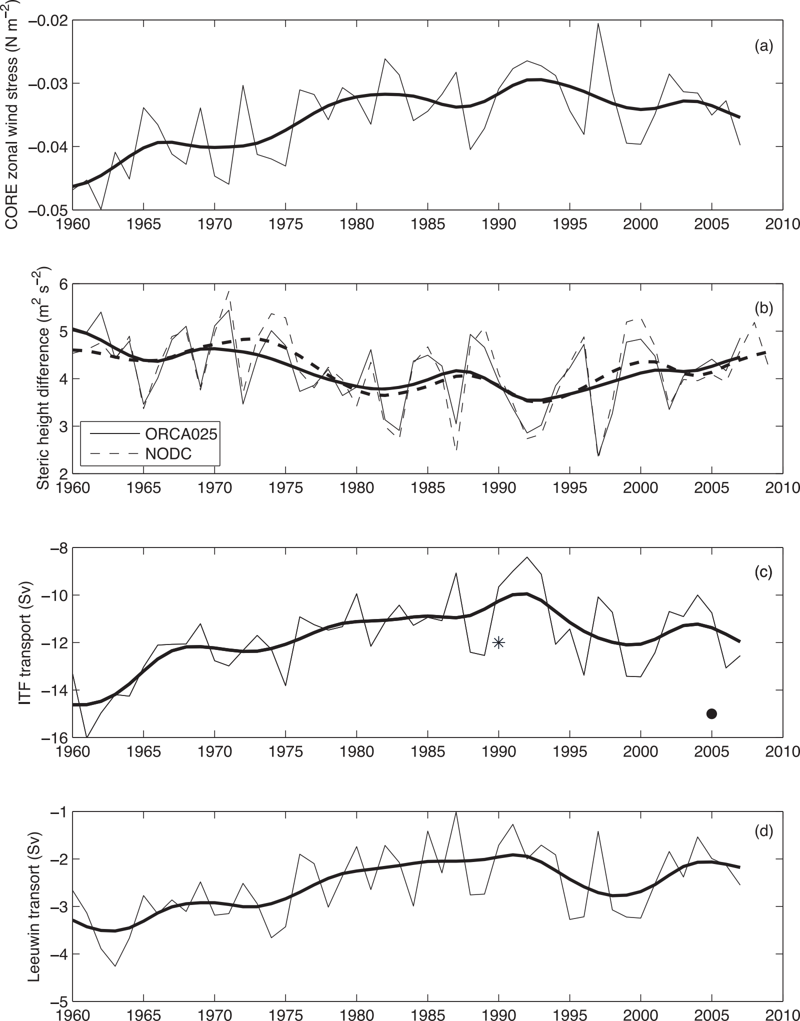

CORE zonal wind stress (N m^{-2})
(a)
−0.02
−0.03
−0.04
−0.05
Steric height difference (m^2 s^{-2})
(b)
ORCA025
NODC
ITF transport (Sv)
(c)
Leeuwin transort (Sv)
(d)
1960
1965
1970
1975
1980
1985
1990
1995
2000
2005
2010